6-2016

Controlling Activity and Selectivity Using Water in the Au-Catalysed Preferential Oxidation of CO in H_2

Johnny Saavedra
Trinity University, jsaaved1@trinity.edu

Todd Whittaker
Trinity University, twhittak@trinity.edu

Zhifeng Chen

Christopher J. Pursell
Trinity University, cpursell@trinity.edu

Robert M. Rioux

See next page for additional authors

Repository Citation

Saavedra, J., Whittaker, T., Chen, Z., Pursell, C. J., Rioux, R. M., & Chandler, B. D. (2016). Controlling activity and selectivity using water in the Au-catalysed preferential oxidation of CO in H_2. *Nature Chemistry*, 8, 584-589. doi: 10.1038/nchem.2494

ARTICLES
PUBLISHED ONLINE: 18 APRIL 2016 | DOI: 10.1038/NCHEM.2494
nature chemistry

Controlling activity and selectivity using water in the Au-catalysed preferential oxidation of CO in H_2

Johnny Saavedra[1,2], Todd Whittaker[1], Zhifeng Chen[3], Christopher J. Pursell[1], Robert M. Rioux[3,4] and Bert D. Chandler[1]*

Industrial hydrogen production through methane steam reforming exceeds 50 million tons annually and accounts for 2–5% of global energy consumption. The hydrogen product, even after processing by the water–gas shift, still typically contains ~1% CO, which must be removed for many applications. Methanation ($CO + 3H_2 \rightarrow CH_4 + H_2O$) is an effective solution to this problem, but consumes 5–15% of the generated hydrogen. The preferential oxidation (PROX) of CO with O_2 in hydrogen represents a more-efficient solution. Supported gold nanoparticles, with their high CO-oxidation activity and notoriously low hydrogenation activity, have long been examined as PROX catalysts, but have shown disappointingly low activity and selectivity. Here we show that, under the proper conditions, a commercial Au/Al_2O_3 catalyst can remove CO to below 10 ppm and still maintain an O_2-to-CO_2 selectivity of 80–90%. The key to maximizing the catalyst activity and selectivity is to carefully control the feed-flow rate and maintain one to two monolayers of water (a key CO-oxidation co-catalyst) on the catalyst surface.

The global chemical industry produces over 50 million tons of hydrogen for several important processes, including ammonia and methanol synthesis, petroleum refining and hydrogenation reactions[1,2]. Hydrogen is produced predominately through a combination of methane steam reforming and water–gas shift reactions; the resulting reformate typically contains about 1% CO in H_2. Many end uses, particularly ammonia synthesis catalysts and fuel cells, are highly sensitive to CO. It must therefore be removed; however, economically removing the last bit of CO has proved challenging. Pressure-swing adsorption requires large capital investments and low flow rates, which reduce throughput and limit H_2 recovery to 70–90%[2]. Methanation ($CO + 3H_2 \rightarrow CH_4 + H_2O$) uses ~5% of the produced H_2, but actual H_2 losses can be up to 10–15% because of the unselective methanation of CO_2 ($CO_2 + 4H_2 \rightarrow CH_4 + 2H_2O$) present in the reformate[2].

The scale of hydrogen production and the potential for preparing hydrogen of fuel-cell grade make hydrogen purification an enormously impactful process. State-of-the-art Pt–Ru catalysts for the fuel-cell anode require CO levels below 50 ppm; economic hydrogen production with lower CO levels may allow for simpler monometallic anode materials[3]. Ammonia production for fertilizer accounts for 2–3% of the total global energy consumption[4], so the use of methanation to purify the hydrogen stream represents an enormous global energy loss. The US National Renewable Energy Laboratory estimates 11.9 kg of CO_2 equivalents are produced for every kilogram of H_2 produced[5]. Consequently, to prevent the (estimated) loss of 1.2 million tons of H_2 used in methanation would eliminate the release of 15 million tons of CO_2 equivalents annually. This is equivalent to saving 35 million barrels of oil per year, or removing more than three million cars from the road[6].

A more-attractive option for hydrogen purification, which could drastically reduce this hydrogen and energy loss, is the preferential oxidation of CO with O_2 (the PROX reaction). A typical benchmark goal for this reaction, which arises primarily from the requirements for a proton-exchange membrane fuel cell, is to reduce the CO concentration at the reactor outlet (hereafter referred to as the 'CO slip') to 50 ppm with O_2 selectivity to CO_2 ≥50%[7–9]. We refer to this as the 50/50 goal. Supported Au nanoparticles are well-known to be highly active CO-oxidation catalysts[10–12] and notoriously poor hydrogenation catalysts[13]. They should be excellent PROX catalysts, but 20 years of research has produced very few catalysts capable of achieving the 50/50 goal (Fig. 1a)[7,14]. Numerous studies have searched for better catalysts, examining particle-size effects[12,15], metal–oxide-support effects[16,17], mixed metal oxides[15,18] and ordered mesoporous materials[19]. Bimetallic catalysts[20], the inclusion of polyoxometallates in liquid-phase media[21], Au–ceria nanocomposites[22] and embedded $Au@CeO_2$ catalysts[23] have also been examined, with limited success.

A general lack of consensus on the CO-oxidation mechanism has hampered catalyst development. Surface hydroxyl groups on the support are clearly necessary for the most-active catalysts[24–26], and we showed[11], following work by the Haruta[27,28], Davis[26,29], Fujitani[30] and Iglesia[31] groups, that water greatly enhances reaction rates. Several groups also suggested that oxygen vacancies on the support play in important mechanistic role[32–34]. More-specific mechanistic PROX investigations by Widmann *et al.* showed that H_2 promotes CO oxidation over Au and the same activated oxygen species is involved in both H_2 and CO oxidation[35]. There is a fairly clear consensus that, for low-temperature CO oxidation, the metal–support interface plays a critical role in the catalysis[11,30,35–38].

We recently proposed a new mechanism for CO oxidation over Au/TiO_2 catalysts, in which water functions as a co-catalyst[11]; the study reported herein applies our newly found mechanistic understanding to CO PROX. Preliminary tests showed that Au/Al_2O_3 catalysts have the same basic CO-oxidation reaction kinetics, and therefore probably operate via the same mechanism (Supplementary Section 3.1) as Au/TiO_2. The Au/Al_2O_3 catalysts were more selective for PROX in our initial testing, so we focused additional studies on this system. Although the promotional effects of water in PROX have been reported[7,39], there is no

[1]Department of Chemistry, Trinity University, San Antonio, Texas 78212-7200, USA. [2]Pacific Northwest National Laboratory, Richland, Washington 99352, USA. [3]Department of Chemical Engineering, The Pennsylvania State University, University Park, Pennsylvania 16802-4400, USA. [4]Department of Chemistry, The Pennsylvania State University, University Park, Pennsylvania 16802-4400, USA. *e-mail: bert.chandler@trinity.edu

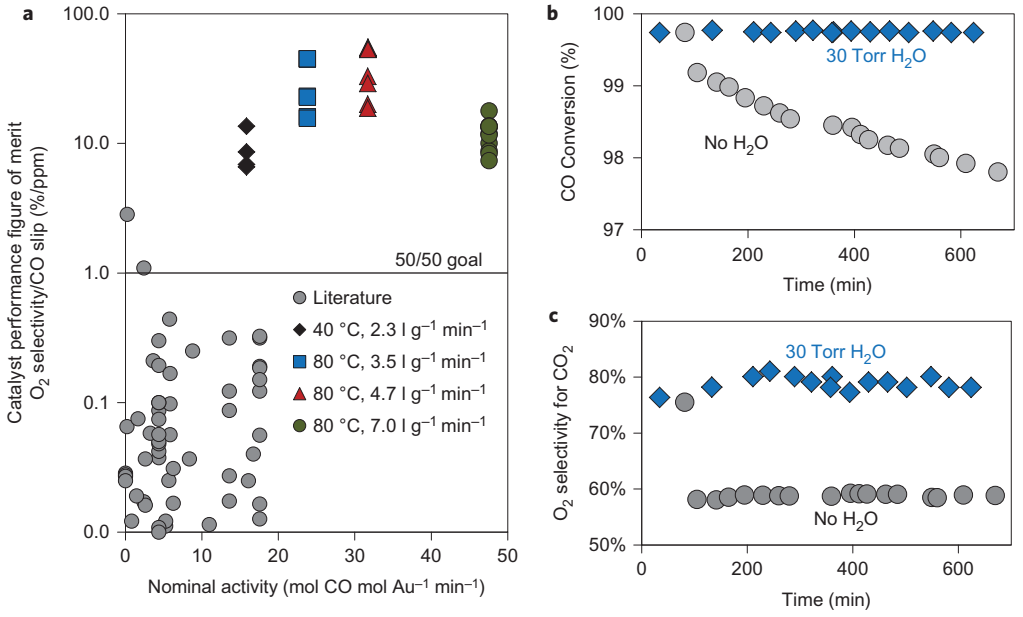

Figure 1 | PROX performance and deactivation of Au/Al_2O_3 with water in the feed (1% CO, 1.4% O_2, 60% H_2, balance He). a, Performance (described by the figure of merit in equation (1)) comparison between Au/Al_2O_3 operated at 40 °C and 80 °C (various SVs, 1–20 Torr H_2O (see Fig. 2)) and literature reports (Supplementary Table 8). When the feed-water content and SV are properly controlled, this Au/Al_2O_3 catalyst far surpasses the literature reports of CO PROX performance, and easily achieves the literature benchmarks. **b**,**c**, CO conversion (**b**) and O_2 selectivity (**c**) during ten hour experiments with Au/Al_2O_3 at 80 °C. When water is removed, the selectivity immediately drops; CO oxidation activity also drops, but more slowly. Thus, maintaining sufficient water on the catalyst prevents deactivation over ten hours, and is critical for optimum catalyst performance. CO-conversion measurements are typically ±0.02%; O_2-selectivity measurements are typically ±5%.

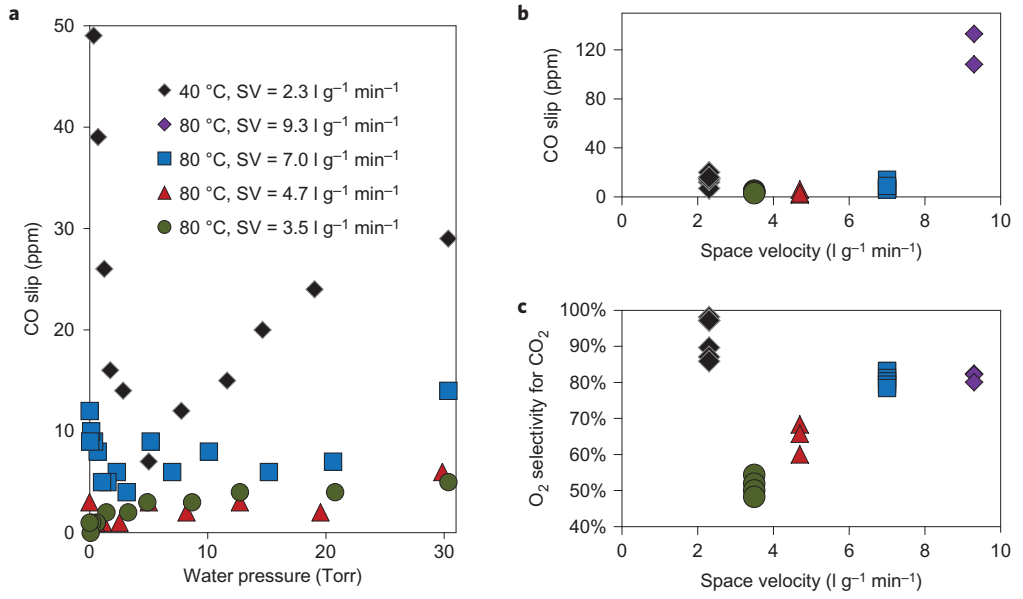

Figure 2 | High conversion PROX reactivity over Au/Al_2O_3. a, CO slip versus P_{H_2O} at several SV values; CO slip is equivalent to the concentration of CO in the reactor outlet. At 40 °C, activity (low CO slip) and selectivity (~90%) are maximized at ~5 Torr added water; CO-oxidation activity increased at 80 °C, but the reaction was less sensitive to added water. **b**, CO slip versus SV for the data in **a**. **c**, O_2 selectivity versus SV for the data in **a**. The data demonstrate that controlling SV can tune the catalyst performance. When the SV is low, very low CO slips (~5 ppm) are achieved, but at the expense of O_2 selectivity. Similarly, if the SV becomes too high, there is insufficient time for the CO to react fully and the CO slip increases. This indicates that the two reactions are essentially sequential: a majority of the CO reacts first, and then the remaining O_2 begins to react with the available H_2. There appears to be a maximum O_2 selectivity of about 80% at 80 °C, which suggests there is insufficient added water.

systematic study that seeks to control the activity and selectivity by adjusting the feed-water content. Herein we show that carefully controlling the feed-water content and space velocity (SV) leads to significant improvements in catalyst performance—far surpassing the 50/50 goal. We also show that the catalyst functions best when the surface coverage of water on the support is about one monolayer and interpret the activity and selectivity gains in terms of our most-recent mechanistic proposal.

Results and discussion

Influence of water on catalyst performance. We studied a commercial Au/Al_2O_3 catalyst, controlling the water content in a model reformate gas stream (Supplementary Section 2.1-3). As catalysts are tested under a wide variety of conditions in various labs, we defined a figure of merit (FOM, Supplementary Section 3.2) to compare efficiently the key aspects of catalyst performance:

$$\mathrm{FOM} = \frac{O_2 \text{ selectivity (\%)}}{\text{CO slip (ppm)}} \quad (1)$$

For reference, a FOM value of one describes a catalyst and reaction conditions that meet the 50/50 goal.

Figure 1a plots several FOM values against the nominal activity for some of our experimental conditions. Approximately 60 literature reports are included (details in Supplementary Section 3.3); most of the data were collected at 80 °C, the operating temperature of many fuel-cell systems[3]. The literature results vary greatly, so the nominal activities are normalized to the total amount of Au, with no adjustments made for Au particle size. We are aware of only two reports that achieve the 50/50 goal, both of which use low SVs and nominally dry feeds[7,14]. By controlling the amount of water added to the reaction (*vide infra*) and using higher SVs, we far surpassed the 50/50 goal, and did so at SVs 1–2 orders of magnitude larger than those in the literature (Fig. 1a and Supplementary Table 8).

Catalyst deactivation is similarly important in PROX, and water may prevent the deposition of carbonates, which poison CO oxidation[8,40,41]. Long-term activity and selectivity plots are shown in Fig. 1b,c, respectively. When water is added to the feed, there is no deactivation over the course of ten hours, and O_2 selectivity remains both constant and high (~80%). When water is removed, O_2 selectivity immediately drops and the CO-oxidation activity begins to degrade over time. These experiments, which employed an unoptimized catalyst, show that huge improvements in PROX performance are possible when the feed-water content is controlled carefully. Furthermore, the potential hydrogen production per unit time is increased by 1–2 orders of magnitude over previous reports, with negligible catalyst deactivation over ten hours.

SV effect. Figure 2 shows CO slip and O_2 selectivity data for the experiments in Fig. 1a. The experimental protocol (Supplementary Section 2.2-3) was critical to achieve a high activity and selectivity, so catalysts were always equilibrated with 30 Torr water before initiating the reaction. The water pressure (P_{H_2O}) was then systematically lowered, which allowed the CO conversion to stabilize at each P_{H_2O} (generally over 30 minutes). To achieve a high activity and selectivity it is critical to control the SV, which is simply the flow rate normalized to the amount of catalyst. When both P_{H_2O} and SV are controlled properly (Fig. 2b,c), the reaction can operate at very high conversions (99.9%, <10 ppm CO slip) and still maintain a high O_2 selectivity (>80%); if the SV drops too low, O_2 selectivity suffers (Fig. 2c).

A SV study at 20 °C (Fig. 3) demonstrated that CO conversion increases as the SV decreases, whereas O_2 selectivity is essentially the same up to 99% CO conversion. Similarly, when CO conversions are high (CO slip ~10 ppm), a decrease in the SV only serves to decrease the O_2 selectivity (Fig. 2b,c; 80 °C). These data indicate that the PROX reaction is largely sequential, with CO reacting before H_2. This conclusion differs somewhat from the most-popular literature mechanisms, which either require H_2 activation to generate the active oxidant[42] or utilize support O atoms[35].

The trends in PROX activity and selectivity, both for our data and much of the PROX literature, can be readily understood in the context of our recently proposed CO-oxidation mechanism for Au/TiO_2 (ref. 11). The key elements of this mechanism are:

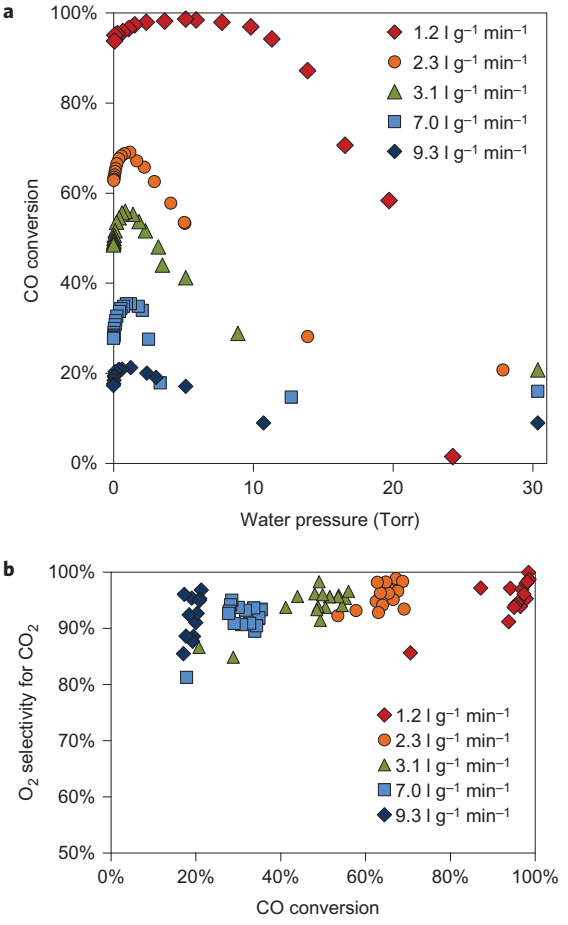

Figure 3 | Effect of SV on CO PROX catalysis over Au/Al_2O_3. **a**, CO conversion as a function of water content at several different values for the SV. **b**, O_2 selectivity for CO_2 as a function of CO conversion at 20 °C. These data show that CO conversion increases as the SV decreases, whereas O_2 selectivity is essentially the same up to a 99% CO conversion. Although there is a small amount of nascent H_2 oxidation at all conversions, the reaction is largely sequential—CO is oxidized first, and then the catalyst begins to oxidize H_2. CO conversion measurements are typically ±0.02%; O_2-selectivity measurements are typically ±5%.

(1) the facile generation of reactive Au–OOH from O_2 and a proton from water adsorbed at the metal–support interface, (2) a very low reaction barrier between Au–OOH and Au–CO and (3) the rate-limiting decomposition of Au–COOH (ref. 11). The CO-oxidation kinetics and H/D kinetic isotope effect for Au/Al_2O_3 are essentially identical to those of Au/TiO_2, which indicates the same mechanism is probably at work (Supplementary Section 3.1). Our results are largely consistent with the extensive PROX mechanistic work from Behm's group[8,35] and Piccolo and co-workers[42]; however, there are two important distinctions from their previous interpretations. First, H_2 activation is not required for the CO-oxidation activity because the active Au–OOH species is derived from O_2 and water. Second, our mechanism does not require the participation of support O, which makes it consistent with isotope-labelling studies in the absence of H_2 (refs 29,31)

Influence of temperature and water coverage. To explore further the roles of water and temperature in PROX, we operated the catalyst under a similar conversion at several temperatures. For each temperature, this necessitated adjusting the SV to achieve a roughly 75% CO conversion at 30 Torr added water. The feed-water content was then decreased systematically. To visualize the trends (Fig. 4a),

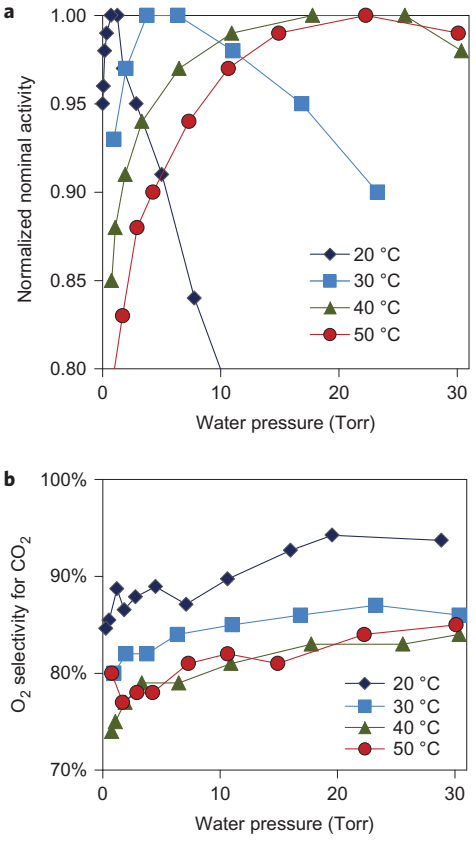

Figure 4 | Effect of water and temperature on CO PROX catalysis over Au/Al_2O_3. a,b, Normalized nominal activity (**a**) and O_2 selectivity for CO_2 (**b**) as functions of P_{H_2O} and temperature. As the reaction temperature increases, the water pressure required to reach the maximum activity shifts to a higher P_{H_2O} and broadens substantially. This suggests that a certain water coverage on the support yields the highest activity. Additionally, the selectivity for CO_2 decreases somewhat as the reaction temperature increases. This is consistent with the mechanistic role of water as a co-catalyst in CO oxidation. Activity measurements are typically ±0.02%; O_2-selectivity measurements are ±5%.

the nominal activity was normalized to the maximum CO conversion at that temperature; associated O_2 selectivity plots are given in Fig. 4b. At 20 °C, Fig. 4a shows a maximum activity at ~2 Torr added water; this value is somewhat lower than the maximum found for CO oxidation in the absence of H_2 (~4–5 Torr (Supplementary Section 3.4)). This is readily explained by the O_2-selectivity data, which show that O_2 selectivity drops at low P_{H_2O}. There are two sources of water in the system—water intentionally added to the inlet feed stream and water produced *in situ* from H_2 oxidation. As Table 1 shows, under the conditions that yield the maximum activity at 20 °C, the water produced *in situ* is important because it accounts for about half of the total water in the system. This explains why so many catalyst reports in the literature show a relatively low activity and O_2 selectivity using dry feeds—in the absence of sufficient surface water, the system oxidizes H_2 to generate the water co-catalyst necessary to oxidize CO. As the amount of water on the support is governed by adsorption–desorption equilibrium and the gas flow constantly removes water from the catalyst surface, the catalyst must constantly oxidize H_2 to maintain a somewhat consistent water coverage on the support. Thus, with insufficient water in the feed, neither high activity nor selectivity is attainable.

The P_{H_2O} range that yields the highest activity increases dramatically as the temperature increases, that is, the peak in Fig. 4a broadens with temperature. This is entirely consistent with the important mechanistic role of water adsorbed on the support because, as the water-adsorption isotherms in Fig. 5a show, as the temperature increases, increasing P_{H_2O} causes a small change in the amount of adsorbed water. To illustrate this, we used the activity and selectivity data from Fig. 4 to estimate the total amount of water in the system (water intentionally added plus water formed by H_2 oxidation) at the activity maximum. This estimate was used along with the adsorption isotherms to estimate the water coverage (θ_{H_2O}) at the activity maximum (Table 1). At each temperature, the maximum activity occurs at about the same θ_{H_2O} (6–9 molecules nm^{-2}), which corresponds to roughly one monolayer of water on the support[43]. This range is illustrated by the box outline in Fig. 5a. This optimum water coverage is compellingly consistent, and is similar to the maximum value found for CO oxidation over Au/TiO_2 (~13 molecules nm^{-2}) (ref. 11).

As Figs 3a and 4a show, if θ_{H_2O} increases above the apparent maximum of approximately one monolayer, then catalytic activity drops. Water binds more strongly to itself than it does to Au (ref. 44); indeed, Au surfaces are considered hydrophobic and require cryogenic experiments to observe water adsorption[45]. This suggests the drop in activity is caused by water that is adsorbed on the support at the metal–support interface physically blocking CO from adsorbing on the Au particles. To test this, we measured CO-adsorption isotherms in the presence of water (Fig. 5b) using infrared spectroscopy[46]. Even in the P_{H_2O} regime in which the activity increases to the maximum value, CO adsorption decreases by 50% relative to the amount adsorbed in the absence of water. Nominal activities for CO oxidation are largely insensitive to CO pressure in this kinetic regime (Supplementary Section 3.1), so physical blocking has little impact on CO-oxidation activity until a very large fraction of the Au sites is blocked.

Beyond the influence on catalytic activity, Figs 1c and 4b clearly show that the addition of water also improves O_2 selectivity. This,

Table 1 | Estimated water content and coverage at maximum PROX activity.

Temperature	20 °C	30 °C	40 °C	50 °C
SV (l g_{cat}^{-1} min^{-1})	2.3	3.5	4.7	9.3
P_{H_2O} at maximum activity*	1.5 Torr	6.1 Torr	17.8 Torr	22.3 Torr
CO conversion	68%	70%	82%	68%
O_2 conversion	28%	30%	35%	30%
O_2 selectivity for CO_2	87%	84%	84%	83%
Total O_2 converted	3,910 ppm	4,170 ppm	4,940 ppm	4,100 ppm
O_2 lost to H_2 oxidation	508 ppm	667 ppm	840 ppm	696 ppm
H_2O produced *in situ*	0.8 Torr	1.0 Torr	1.3 Torr	1.0 Torr
Estimated total P_{H_2O}	2.3 Torr	7.1 Torr	19 Torr	23 Torr
Adsorbed H_2O†	2.4 mmol g^{-1}	3.1 mmol g^{-1}	3.5 mmol g^{-1}	2.7 mmol g^{-1}
θ_{H_2O} (molecules nm^{-2})‡	6.1	7.6	8.9	7.1

*From Fig. 4a. Feed: 10,000 ppm (1%) CO, 14,000 ppm (1.4%) O_2, variable water, 60% H_2, balance He. †Estimated from the total P_{H_2O} and water-adsorption isotherms (Fig. 5a). ‡Based on the N_2 BET (Brunauer, Emmett and Teller) surface area.

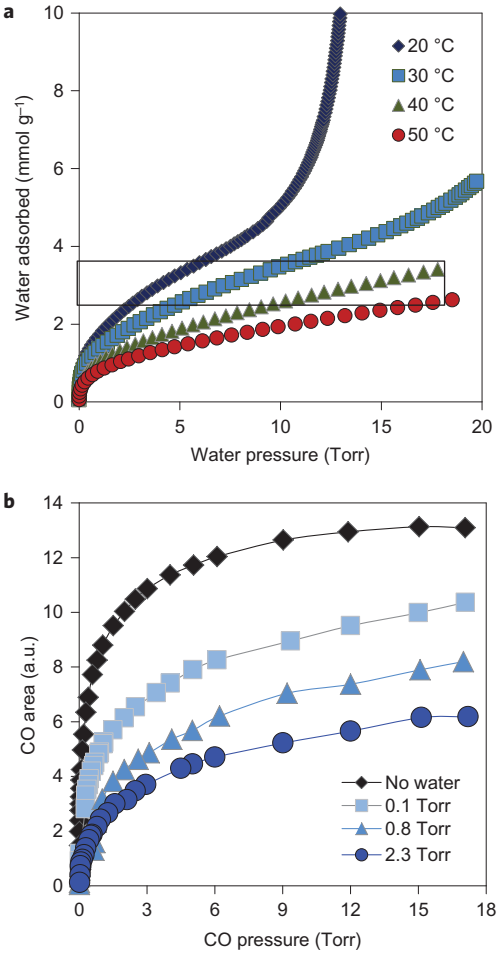

Figure 5 | Gas-adsorption data. a, Volumetric water-adsorption isotherms (20–50 °C) on the Au/Al_2O_3 catalyst. As the temperature increases, the amount of water adsorbed on the catalyst at a given pressure decreases substantially. The box indicates the range of θ_{H_2O} that corresponds to the activity maxima in Fig. 4a and Table 1. A relatively narrow range of water coverage enables the highest CO-oxidation activity, regardless of the reaction temperature. **b**, CO-adsorption isotherms (20 °C) determined by infrared spectroscopy in the presence and absence of water. At pressures as low as 2.3 Torr, at which total CO oxidation activity is maximized, roughly half of the CO-adsorption sites are blocked by water. This is presumably because of the physical blocking of the adsorption sites at the metal–support interface by water adsorbed on the support. Errors in adsorption-isotherm measurements are typically ±5%. a.u., arbitrary units.

too, can be understood in the context of our recently proposed reaction mechanism for CO oxidation[11]. The P_{H_2O} and SV studies indicate that the reaction is largely sequential, such that most of the CO is consumed before H_2 is oxidized. This suggests catalyst selectivity is largely determined by the competition between adsorbed CO and H_2 for the Au–OOH intermediate. Spectroscopic evidence for peroxo and superoxo species stabilized on the support have been reported for Au/CeO_2 catalysts[47]. CO binds to Au much more strongly than does H_2, so the CO coverage is expected to be high relative to the H_2 coverage, even under excess H_2. When the reaction is pushed to a very high CO conversion (Fig. 2), towards the bottom of the catalyst bed there are sufficient Au sites available for H_2 to react. Thus, the SV, conversion and water coverage control the fraction of Au sites available to catalyse H_2 oxidation.

There may also be kinetic influences on the high selectivity. Our previous density functional theory study found a very low reaction barrier (0.1 eV) for Au–CO reacting with Au–OOH (ref. 11). Hydrogen chemisorption on Au is an activated process[48], which suggests that at a low temperature this may be slow relative to CO activation. The general trend of decreasing O_2 selectivity as temperature increases (Fig. 4b) is also consistent with a H_2 adsorption/reaction with Au–OOH having a larger activation barrier.

At all the temperatures studied, PROX selectivity generally increased with P_{H_2O} (Fig. 4b). Behm's group showed that CO and H_2 compete for a common reactive oxygen intermediate[35], which indicates that water has a larger effect in blocking H_2-adsorption sites than it does in blocking CO sites (Fig. 4b). As water is adsorbed on the support, this is consistent with the conclusion that H_2-adsorption/activation sites are located at the metal–support interface[35,36,42]. This provides an interesting positive feedback loop—when water coverage is low, H_2 oxidation begins to produce water, which accelerates CO oxidation. This interpretation is largely consistent with the bulk of the PROX mechanistic literature, and explains why previous studies have not successfully achieved the 50/50 goal.

Our results show that an unoptimized catalyst can be a commercially viable H_2-purification catalyst provided the SV, θ_{H_2O} and reaction temperature are controlled carefully. Understanding the fundamental steps in the reaction mechanism essentially turns this from a catalyst optimization problem to one of reaction engineering. Controlling SV and θ_{H_2O} essentially allows us to tune the number of available active sites, which allows adjustments for differing feeds. This is a substantial advantage, and potentially allows us to uncover additional active sites as a catalyst begins to deactivate over time (for example, because of sulfur poisoning). For wet feeds, this may be accomplished simply by cooling to a temperature at which the water vapour pressure is close to the P_{H_2O} required for the maximum catalytic activity.

This is not to say that the catalyst cannot or should not be optimized; rather, the mechanistic understanding provides similarly clear directions as to how the catalyst can be improved or tuned for specific conditions. Balancing the water-binding properties of the support with the feed-water content is likely to be important. Supports that bind water more tightly will be desirable for relatively dry feeds—this should reduce the need to add water to the system; conversely, supports that bind water weakly will probably be better for wet feeds. Selectivity improvements should arise from tuning the CO- and H_2-binding properties of Au, as Bond *et al.* suggested[13]. Any electronic effects (for example, support effects, particle-size effects or promoters) that increase the CO-adsorption energy relative to the H_2-adsorption energy should provide for a greater differentiation between the two reactants and a higher selectivity.

Methods

Further details are available in the Supplementary Information. Catalysis experiments were performed in a single-pass plug-flow microreactor. The reaction zone consisted of finely ground fresh catalyst (5–100 mg) diluted in SiC (1,200 mg). Gas flows were controlled with electronic mass-flow controllers. The gas-feed (1% CO, 1.4% O_2, 60% H_2, balance He 140 ml min^{-1}; SV = 1.4–28 l g^{-1} min^{-1}) and reactor-effluent compositions were determined using a Siemens Ultramat 23 infrared gas analyser. Moisture (0.1–30 Torr) was added to the feed with a water saturator immersed in a cooling bath. The reaction temperature (20–80 °C) was maintained with a water bath and recirculating water pump. The catalyst was first stabilized in the wettest reactive atmosphere until steady-state conditions were reached. The feed-water pressure was then decreased by decreasing the saturator-bath temperature.

CO-adsorption infrared experiments were performed as described previously[49]. Approximately 25 mg of the sample were pressed into a 30 × 30 mesh Ti wire cloth (Unique Wire Weaving Co.) and mounted into a custom-built copper cell and vacuum chamber with a gas-phase optical-path length of 1.2 cm. The sample was first dried under vacuum at room temperature and a background spectrum was recorded. CO (20 Torr) was added to the cell and allowed to equilibrate for 5–10 minutes. Once at equilibrium, an infrared spectrum was collected. The CO pressure was then decreased incrementally and infrared spectra were collected at each equilibrated CO pressure. The cell was then evacuated, 0.1 Torr water was added to the chamber and allowed to equilibrate. CO was then added incrementally to the chamber and infrared spectra were collected at each CO pressure. This general procedure was repeated for higher water pressures.

Water-adsorption isotherms were measured at four different temperatures (20, 30, 40 and 50 °C) using a Micromeritics 3Flex volumetric adsorption apparatus.

Details of the sample pretreatment are given in Supplementary Section 2.7. The sample temperature was maintained using a Neslab recirculating bath coupled to a Cryofab Dewar. The water-source temperature was maintained at 43 ± 0.1 °C and the instrument manifold was maintained at 45 ± 0.02 °C. During the measurements, small doses of water (0.05 mmol g^{-1}) were equilibrated with the sample to develop high-resolution adsorption and desorption isotherms.

Received 1 May 2015; accepted 8 March 2016; published online 18 April 2016

References

1. Neef, H. J. International overview of hydrogen and fuel cell research. *Energy* **34,** 327–333 (2009).
2. Liu, K., Song, C. & Subramani, V. *Hydrogen and Syngas Production and Purification Technologies* (John Wiley & Sons, Inc., 2010).
3. Ghenciu, A. F. in *Fuel Cells Compendium* (eds Brandon, N. & Thompsett, D.) Ch. 5, 91–106 (Elsevier, 2005).
4. European Commission *Best Available Techniques for the Manufacture of Large Volume Inorganic Chemicals – Ammonia, Acids and Fertilisers* (European Commission, 2007).
5. Spath, P. L. & Mann, M. K. *Life Cycle Assessment of Hydrogen Production via Natural Gas Steam Reforming* (Department of Energy, National Renewable Energy Laboratory, 2001).
6. *Greenhouse Gas Emissions Calculations and References* (US Environment Protection Agency, 2015); www.epa.gov/energy/ghg-equivalencies-calculator-calculations-and-references
7. Landon, P. *et al.* Selective oxidation of CO in the presence of H_2, H_2O and CO_2 utilising Au/α-Fe_2O_3 catalysts for use in fuel cells. *J. Mater. Chem.* **16,** 199–208 (2006).
8. Schumacher, B., Denkwitz, Y., Plzak, V., Kinne, M. & Behm, R. J. Kinetics, mechanism, and the influence of H_2 on the CO oxidation reaction on a Au/TiO_2 catalyst. *J. Catal.* **224,** 449–462 (2004).
9. Lakshmanan, P., Park, J. & Park, E. Recent advances in preferential oxidation of CO in H_2 over gold catalysts. *Catal. Surv. Asia* **18,** 75–88 (2014).
10. Green, I. X., Tang, W., Neurock, M. & Yates, J. T. Jr. Spectroscopic observation of dual catalytic sites during oxidation of CO on a Au/TiO_2 catalyst. *Science* **333,** 736–739 (2011).
11. Saavedra, J., Doan, H. A., Pursell, C. J., Grabow, L. C. & Chandler, B. D. The critical role of water at the gold–titania interface in catalytic CO oxidation. *Science* **345,** 1599–1602 (2014).
12. Valden, M., Lai, X. & Goodman, D. W. Onset of catalytic activity of gold clusters on titania with the appearance of nonmetallic properties. *Science* **281,** 1647–1650 (1998).
13. Bond, G. C., Louis, C. & Thompson, D. T. *Catalysis by Gold* Vol. 6 (Imperial College Press, 2006).
14. Avgouropoulos, G. *et al.* A comparative study of Pt/γ-Al_2O_3, Au/α-Fe_2O_3 and CuO–CeO_2 catalysts for the selective oxidation of carbon monoxide in excess hydrogen. *Catal. Today* **75,** 157–167 (2002).
15. Grisel, R. J. H. & Nieuwenhuys, B. E. Selective oxidation of CO, over supported Au catalysts. *J. Catal.* **199,** 48–59 (2001).
16. Ivanova, S., Pitchon, V., Petit, C. & Caps, V. Support effects in the gold-catalyzed preferential oxidation of CO. *ChemCatChem* **2,** 556–563 (2010).
17. Widmann, D., Liu, Y., Schueth, F. & Behm, R. J. Support effects in the Au-catalyzed CO oxidation—correlation between activity, oxygen storage capacity, and support reducibility. *J. Catal.* **276,** 292–305 (2010).
18. Tompos, A. *et al.* Role of modifiers in multi-component MgO-supported Au catalysts designed for preferential CO oxidation. *J. Catal.* **266,** 207–217 (2009).
19. Liu, Y. *et al.* Three-dimensionally ordered macroporous Au/CeO_2–Co_3O_4 catalysts with mesoporous walls for enhanced CO preferential oxidation in H_2-rich gases. *J. Catal.* **296,** 65–76 (2012).
20. Li, X. *et al.* Activation and deactivation of Au-Cu/SBA-15 catalyst for preferential oxidation of CO in H_2-rich gas. *ACS Catal.* **2,** 360–369 (2012).
21. Kim, W. B., Voitl, T., Rodriguez-Rivera, G. J., Evans, S. T. & Dumesic, J. A. Preferential oxidation of CO in H_2 by aqueous polyoxometalates over metal catalysts. *Angew. Chem. Int. Ed.* **44,** 778–782 (2005).
22. Carrettin, S., Concepcion, P., Corma, A., Lopez Nieto, J. M. & Puntes, V. F. Gold catalysts: nanocrystalline CeO_2 increases the activity of Au for CO oxidation by two orders of magnitude. *Angew. Chem. Int. Ed.* **43,** 2538–2540 (2004).
23. Cargnello, M. *et al.* Active and stable embedded Au@CeO_2 catalysts for preferential oxidation of CO. *Chem. Mater.* **22,** 4335–4345 (2010).
24. Singh, J. A., Overbury, S. H., Dudney, N. J., Li, M. & Veith, G. M. Gold nanoparticles supported on carbon nitride: influence of surface hydroxyls on low temperature carbon monoxide oxidation. *ACS Catal.* **2,** 1138–1146 (2012).
25. Ketchie, W. C., Murayama, M. & Davis, R. J. Promotional effect of hydroxyl on the aqueous phase oxidation of carbon monoxide and glycerol over supported Au catalysts. *Top. Catal.* **44,** 307–317 (2007).
26. Ide, M. S. & Davis, R. J. The important role of hydroxyl on oxidation catalysis by gold nanoparticles. *Acc. Chem. Res.* **47,** 825–833 (2014).
27. Date, M. & Haruta, M. Moisture effect on CO oxidation over Au/TiO_2 catalyst. *J. Catal.* **201,** 221–224 (2001).
28. Date, M., Okumura, M., Tsubota, S. & Haruta, M. Vital role of moisture in the catalytic activity of supported gold nanoparticles. *Angew. Chem. Int. Ed.* **43,** 2129–2132 (2004).
29. Calla, J. T. & Davis, R. J. Oxygen-exchange reactions during CO oxidation over titania- and alumina-supported Au nanoparticles. *J. Catal.* **241,** 407–416 (2006).
30. Fujitani, T. & Nakamura, I. Mechanism and active sites of the oxidation of CO over Au/TiO_2. *Angew. Chem. Int. Ed.* **50,** 10144–10147 (2011).
31. Ojeda, M., Zhan, B.-Z. & Iglesia, E. Mechanistic interpretation of CO oxidation turnover rates on supported Au clusters. *J. Catal.* **285,** 92–102 (2012).
32. Widmann, D. & Behm, R. J. Activation of molecular oxygen and the nature of the active oxygen species for CO oxidation on oxide supported Au catalysts. *Acc. Chem. Res.* **47,** 740–749 (2014).
33. Kung, M. C., Davis, R. J. & Kung, H. H. Understanding Au-catalyzed low-temperature CO oxidation. *J. Phys. Chem. C* **111,** 11767–11775 (2007).
34. Haruta, M. Spiers Memorial Lecture. Role of perimeter interfaces in catalysis by gold nanoparticles. *Faraday Discuss.* **152,** 11–32 (2011).
35. Widmann, D., Hocking, E. & Behm, R. J. On the origin of the selectivity in the preferential CO oxidation on Au/TiO_2—nature of the active oxygen species for H_2 oxidation. *J. Catal.* **317,** 272–276 (2014).
36. Fujitani, T., Nakamura, I., Akita, T., Okumura, M. & Haruta, M. Hydrogen dissociation by gold clusters. *Angew. Chem. Int. Ed.* **48,** 9515–9518 (2009).
37. Cargnello, M. *et al.* Control of metal nanocrystal size reveals metal–support interface role for ceria catalysts. *Science* **341,** 771–773 (2013).
38. Kotobuki, M., Leppelt, R., Hansgen, D. A., Widmann, D. & Behm, R. J. Reactive oxygen on a Au/TiO_2 supported catalyst. *J. Catal.* **264,** 67–76 (2009).
39. Schubert, M. M., Venugopal, A., Kahlich, M. J., Plzak, V. & Behm, R. J. Influence of H_2O and CO_2 on the selective CO oxidation in H_2-rich gases over Au/α-Fe_2O_3. *J. Catal.* **222,** 32–40 (2004).
40. Saavedra, J., Powell, C., Panthi, B., Pursell, C. J. & Chandler, B. D. CO oxidation over Au/TiO_2 catalyst: pretreatment effects, catalyst deactivation, and carbonates production. *J. Catal.* **307,** 37–47 (2013).
41. Denkwitz, Y. *et al.* Stability and deactivation of unconditioned Au/TiO_2 catalysts during CO oxidation in a near-stoichiometric and O_2-rich reaction atmosphere. *J. Catal.* **251,** 363–373 (2007).
42. Quinet, E. *et al.* On the mechanism of hydrogen-promoted gold-catalyzed CO oxidation. *J. Catal.* **268,** 384–389 (2009).
43. Carrasco, J., Hodgson, A. & Michaelides, A. A molecular perspective of water at metal interfaces. *Nature Mater.* **11,** 667–674 (2012).
44. Gong, J. Structure and surface chemistry of gold-based model catalysts. *Chem. Rev.* **112,** 2987–3054 (2011).
45. Ikemiya, N. & Gewirth, A. A. Initial stages of water adsorption on Au surfaces. *J. Am. Chem. Soc.* **119,** 9919–9920 (1997).
46. Pursell, C. J., Hartshorn, H., Ward, T., Chandler, B. D. & Boccuzzi, F. Application of the Temkin model to the adsorption of CO on gold. *J. Phys. Chem. C* **115,** 23880–23892 (2011).
47. Guzman, J., Carrettin, S. & Corma, A. Spectroscopic evidence for the supply of reactive oxygen during CO oxidation catalyzed by gold supported on nanocrystalline CeO_2. *J. Am. Chem. Soc.* **127,** 3286–3287 (2005).
48. Bus, E., Miller, J. T. & van Bokhoven, J. A. Hydrogen chemisorption on Al_2O_3-supported gold catalysts. *J. Phys. Chem. B* **109,** 14581–14587 (2005).
49. Hartshorn, H., Pursell, C. J. & Chandler, B. D. Adsorption of CO on supported gold nanoparticle catalysts: a comparative study. *J. Phys. Chem. C* **113,** 10718–10725 (2009).

Acknowledgements

The authors kindly thank J. Kenvin (Micromeritics Instrument Corporation) and S.M.K. Shahri (Pennsylvania State University) for assistance with the measurement of the water-adsorption isotherms. The authors gratefully acknowledge the US National Science Foundation (Grant No CBET-1160217 and No. CHE-1012395) for financial support of this work. Z.C. and R.M.R. acknowledge the Department of Energy, Office of Basic Energy Sciences, Chemical Sciences, Geosciences, and Biosciences Division, Catalysis Sciences Program under grant No. DE-FG02-12ER16364 for partial funding of this research.

Author contributions

J.S., B.D.C. and C.J.P. designed the catalysis experiments; J.S. performed the catalysis experiments and analysed the data; B.D.C. and C.J.P. designed the infrared spectroscopy experiments; T.W. performed the infrared spectroscopy experiments and analysed the data; B.D.C. and R.M.R. designed the gas-adsorption experiments and analysed the data; Z.C. and R.M.R. designed and performed the X-ray photoemission spectroscopy and X-ray diffraction experiments (see the Supplementary Information) and analysed the data; J.S., B.D.C., R.M.R. and C.J.P. co-wrote the paper.

Additional information

Supplementary information is available in the online version of the paper. Reprints and permissions information is available online at www.nature.com/reprints. Correspondence and requests for materials should be addressed to B.D.C.

Competing financial interests

The authors declare no competing financial interests.